Thin Solid Films 645 (2018) 102–107

Contents lists available at ScienceDirect

Thin Solid Films

journal homepage: www.elsevier.com/locate/tsf

Reduction of defect states in atomic-layered HfO_2 film on SiC substrate using post-nitridation annealing

Sera Kwon[a], Dae-Kyoung Kim[b], Mann-Ho Cho[b], Kwun-Bum Chung[a,*]

[a] Division of Physics and Semiconductor Science, Dongguk University, Seoul 100-715, Republic of Korea
[b] Institute of Physics and Applied Physics, Yonsei University, Seoul 120-749, Republic of Korea

ARTICLE INFO

Keywords:
HfO2
Defect states
Atomic layer deposition
Post-nitridation annealing
SiC

ABSTRACT

The changes of the defect states below the conduction band in atomic-layered HfO_2 film grown on SiC substrate were examined as a function of the post-nitridation annealing temperature in an NH_3 ambient. As the post-nitridation annealing temperature increased up to 600 °C, the incorporated nitrogen into the HfO_2/SiC interface was gradually increased. The band gap and valence band offset were mostly increased as a function of the post-nitridation annealing temperature and the band alignment of HfO_2 films changed. O K-edge absorption features revealed two distinct band edge states below the conduction band edge in HfO_2 films, and these defect states were dramatically reduced with increasing of the post-nitridation annealing temperature. The reduction of defect states in HfO_2/SiC improved the electrical properties such as the leakage current density, breakdown voltage, and trap charge density in the HfO_2 film and interface of HfO_2/SiC.

1. Introduction

Silicon carbide (SiC) has been attracted as a promising material for the next-generation high power metal-oxide-semiconductor (MOS)-based devices because of the wide bandgap (~3.26 eV for 4H-SiC), a high thermal conductivity (4.9 W/cm·°C), and a high electric breakdown field (2.5–3.5 MV/cm) that provide a performance that is superior to that of Si [1,2,3,4]. Also, a significant advantage of SiC is an ability whereby high quality silicon dioxide (SiO_2) layers that deliver a performance that is similar to that of Si can be grown through thermal oxidation [5]. However, the electrical properties of the traditional SiO_2 that is grown on the SiC substrate are reduced, regardless of the electrically excellent properties of SiC, due to a low dielectric constant [6]. To solve this problem, a number of research studies have reported the application of gate oxides with high dielectric constant (high-*k*) that suppress the electric field across the gate dielectric by a high *k*-factor compared to SiO_2 (~3.9) for the same electric field [7,8]. Among the high-*k* oxide materials, HfO_2 has attracted great interest as an insulating material for devices due to a high dielectric constant (~25) and a superior chemical and thermal stability, therefore, the electrical limitation could be solved through the use of the HfO_2 insulating layer instead of SiO_2 [9]. However, the relatively high defect densities such as the interfacial dangling bond, oxygen vacancies, and carbon cluster at the high-*k* oxide/SiC interface result in the degradation of the electrical characteristics [10,11]. The defect states at the high-*k* oxide/SiC interface act as electrical traps that influence the frequency dispersion and the device reliability. Regarding a high-*k* oxide/SiC interface that includes nitrogen, several research groups have discussed the characteristics of the interfacial defect states in a nitric-oxide ambient (NO_x) such as implantation, plasma treatment, and thermal-annealing [12,13,14,15]. In particular, NO_x ambient treatment, which reduces the interface defect density at the high-k oxide/SiC interface, has been commonly used over the past decade [16,17]. Despite of the advantage of the NO_x treatment, this method leads to the disturbance of the nitrogen insertion due to the presence of excess oxygen, and as a result, the excess oxygen can result in additional defect formations [18,19]. An alternative nitridation method for which NOx is used involves the use of ammonia (NH_3) gas, and it is an effective method for the removal of the dangling bond and the carbon cluster for which additional forming gas annealing is not required, accordingly, this method could be more suitable for more complicated surface geometries [20]. An understanding of the role of nitrogen at the high-*k* oxide/SiC interface is therefore very important, as it critically related to the changes of the electronic structures.

In this study, the nitrogen incorporation effect in HfO_2/SiC is reported with the use of thermal annealing in the NH_3 ambient and as a function of the post-nitridation temperature. The energy band gap and the band offset were changed through the nitrogen incorporation at the HfO_2/SiC interface. The quantitative changes of the two distinct band edge defects below the conduction band in the defect states were

* Corresponding author.
E-mail address: kbchung@dongguk.edu (K.-B. Chung).

http://dx.doi.org/10.1016/j.tsf.2017.10.020
Received 2 February 2017; Received in revised form 9 October 2017; Accepted 9 October 2017
Available online 12 October 2017

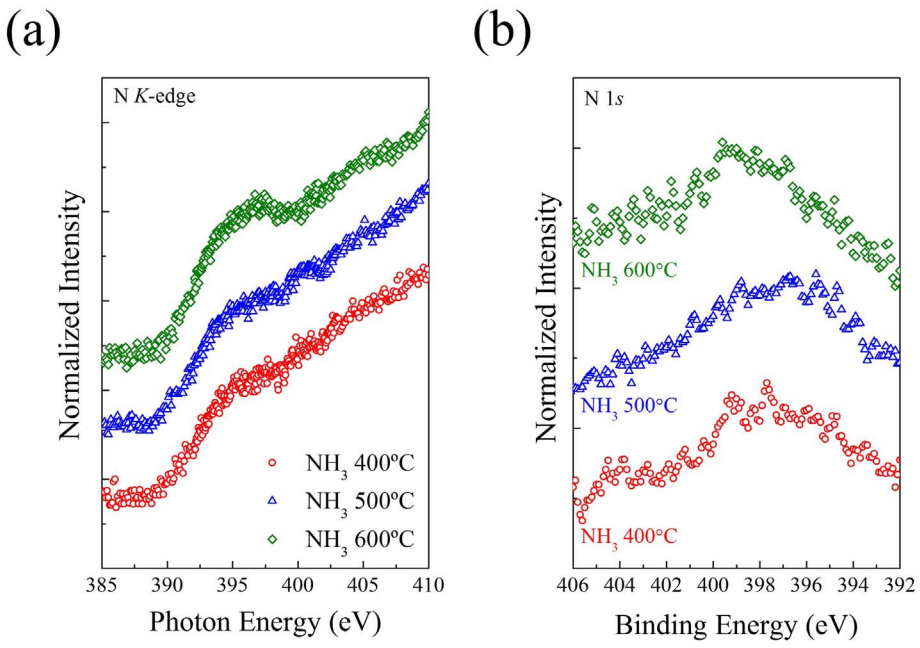

Fig. 1. (a) N-K edge absorption spectra and (b) XPS spectra of N 1*s* core-level as a function of the post-nitridation temperature.

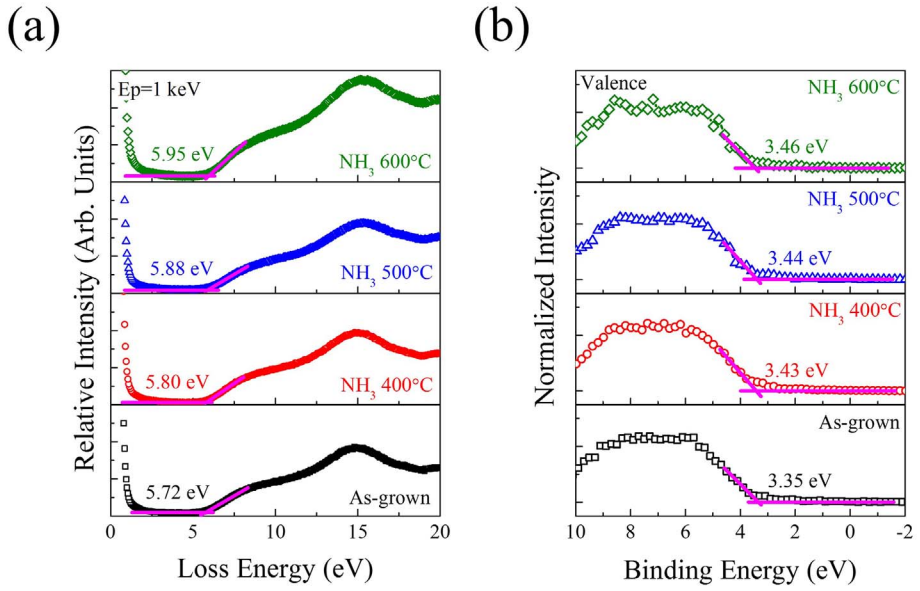

Fig. 2. (a) REELS spectra with primary energy of 1.0 keV and (b) valence band spectra as a function of the post-nitridation temperature.

Table 1
The band gap, the valence band maximum (VBM), the conduction band minimum (CBM) of the HfO_2, and the band offset between the HfO_2 and the SiC as a function of the post-nitridation treatment from the REELS and the valence band spectra.

Temperature (°C)	E_g (eV)	VBM (eV)	CBM (eV)	ΔE_{VB} (eV)	ΔE_{CB} (eV)
As-grown	5.72	3.35	2.37.	1.69	0.90
400	5.80	3.43	2.37	1.77	0.90
500	5.88	3.44	2.44	1.78	0.97
600	5.95	3.46	2.49	1.80	1.02

strongly correlated to the electrical characteristics such as the leakage current density, breakdown voltage, and effective trap charge density. These results indicate that the post-annealing treatments in the NH_3 ambient clearly improve the interfacial properties of the HfO_2/SiC.

2. Experiment

The HfO_2 films were deposited on a n-type 4H-SiC (0001) with a carrier concentration of $\sim 5 \times 10^{18}$ cm^{-3}. Prior to the deposition of the HfO_2 films, the SiC wafers were cleaned with hydrofluoric acid treatment to remove the native oxide from the surface. Then, 5-nm HfO_2 films were immediately deposited using the atomic layer deposition (ALD) process, thereby tetrakis-ethyl-methyl-amide hafnium $Hf[N(CH_3)(C_2H_5)]_4$ (TEMAHf) was used as the hafnium precursor and H_2O vapor was used as the oxygen source. One cycle for the deposition of the HfO_2 comprised 1 s of the TEMAHf feeding, 20 s of the N_2 purge, 1.5 s of the H_2O feeding, and 30 s of the N_2 purge at the substrate temperature of 250 °C. After the deposition process, the HfO_2 films were annealed by a rapid thermal process (RTP) for 1 min at each of the temperature 400, 500, and 600 °C in the ambient of NH_3 gas. The valence band offset and chemical bonding states of the HfO_2/SiC were measured with X-ray photoelectron spectroscopy (XPS) using a monochromatic Al Kα X-ray source ($h\nu$ = 1486.7 eV). To eliminate the carbon contamination on the

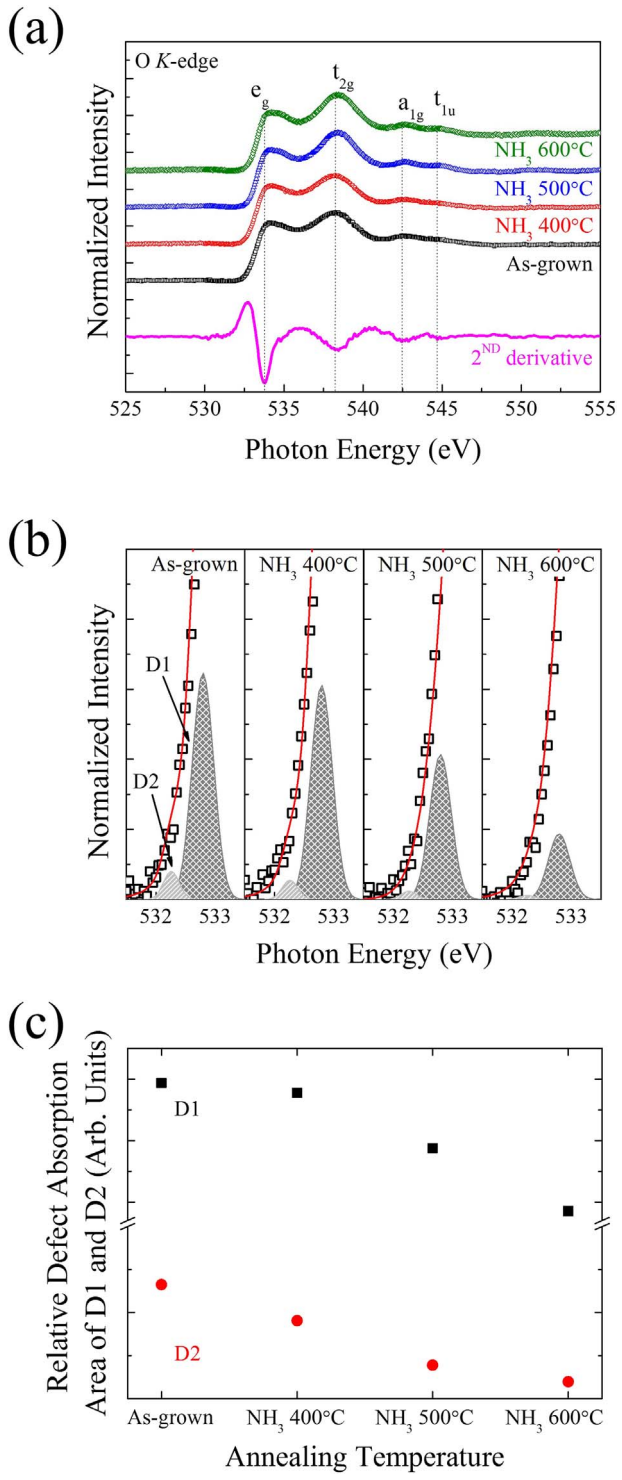

Fig. 3. (a) Normalized O K-edge absorption spectra with second-derivative O *K*-edge spectrum at the bottom of the figure, (b) deconvoluted defect states below the conduction band edge from the use of the Gaussian fits, and (c) relative defect absorption area of the two distinct band edge states (D1 and D2) as a function of the post-nitridation temperature.

surface, an Ne-ion sputtering was performed for 1 min prior to the XPS measurement at the sputtering power of 1 kV. To assess the changes of the energy band gap of the HfO_2 films as a function of the post-annealing temperature of the HfO_2 films, reflection electron energy loss spectroscopy (REELS) measurement was carried out with a primary electron beam energy of 1.0 keV, and the HfO_2 film surface was sputtered with an Ar-ion for 1 min at a sputtering power of 0.5 keV. The changes of the electronic structures that are related to the conduction band and the band edge state below the conduction band were investigated with X-ray absorption spectroscopy (XAS) at the 10D beam line facility, Pohang Accelerator Laboratory (PAL), Korea. To fabricate the metal-oxide-semiconductor capacitor (MOSCAP) for analysis the electrical characteristics, 100-nm-thick platinum electrodes were deposited on the HfO_2/SiC via a photolithography process for which wet chemical etching was performed regarding the metal. The electrical properties such as the leakage current density, breakdown voltage, capacitance, and hysteresis were obtained with the use of the measurements of the leakage current density-voltage (J-V) and the capacitance-voltage (C-V) as a function of the temperature of the post-annealing treatment in the NH_3 ambient.

3. Results and discussion

To verify the existence of nitrogen within the HfO_2 film and/or the HfO_2/SiC interface, the N K-edge absorption spectra and the N 1*s* core-level spectra that correspond to the HfO_2/SiC samples as a function of the post-nitridation temperature were investigated and are shown in Fig. 1 (a) and (b), respectively. The N K-edge absorption spectra revealed the chemical state of the nitrogen in the HfO_2 film. As shown in Fig. 1 (a), the broad feature near 400 eV gradually appeared as the post-nitridation temperature increased up to 600 °C, while the sharp feature related to the resonant excitations of the N_2 molecule states was not evident. The broad feature is related to the hybridized orbital structure of the Hf 6*sp* + N 2*p* states, or it is caused by the Si 3*sp* + N 2*p* states because of the interaction of the nitrogen atoms at the HfO_2/SiC interface [21,22]. Fig. 1 (b) shows the N 1*s* core-level spectra as a function of the post-nitridation temperature. The use of the N 1*s* spectra for an accurate examination of the nitrogen bonding states is difficult because the N 1*s* spectrum is close to the Hf 4*p* spectrum, however, the intensity of the N 1*s* slightly increased as a function of the post-nitridation temperature, which could mean that the quantity of nitrogen that was incorporated into the HfO_2 film and interface of HfO_2/SiC increased gradually with the increasing of the post-nitridation temperature.

The energy band gap (E_g) for the HfO_2/SiC as a function of the post-nitridation temperature, as shown in Fig. 2 (a), was determined with the use of REELS. The E_g value was slightly increased after the post-nitridation treatment up to 5.95 eV in the post-nitridated HfO_2 film at 600 °C. This tendency is considered that the formation of an interfacial layer like HfSiON from the incorporation of nitrogen into the HfO_2/SiC interface. Because the E_g value in the SiON layer is dependent upon the quantity of the nitrogen incorporation, commonly E_g value is indicated to ~7.0 eV in the NH_3 ambient [23]. Fig. 2 (b) shows the valence band spectra in the XPS that provide the energy level difference between the Fermi level and the valence band maximum (VBM) in the HfO_2 film. Moreover, from the results of E_g and the VBM, the conduction band minimum (CBM) was also calculated as shown in Table 1. The E_g and the VBM for the SiC substrate were determined with the use of spectroscopic ellipsometry (SE) and the valence band spectra in the XPS, respectively, and the obtained values were 3.13 eV, and 1.66 eV, respectively (not shown here). The most important finding is that the change of the band offset between the HfO_2 and the SiC substrate was dependent on the post-nitridation temperature. The value of the valence band offset (ΔE_{VB}) gradually increased as the post-annealing temperature was increased up to 600 °C, and the ΔE_{VB} of the as-grown HfO_2 films of 1.69 eV increased to 1.80 eV at the post-nitridation temperature of 600 °C. Likewise, the ΔE_{CB} value was increased from 0.90 eV to 1.02 eV. Based on the previous XAS and XPS spectra, the changes of the band alignment could be associated with the interfacial reaction that is from the incorporation of nitrogen.

To understand the electronic structure for the post-nitridation treatment of the HfO_2/SiC, the O K-edge absorption spectra were investigated, as shown in Fig. 3 (a). The qualitative analysis of the

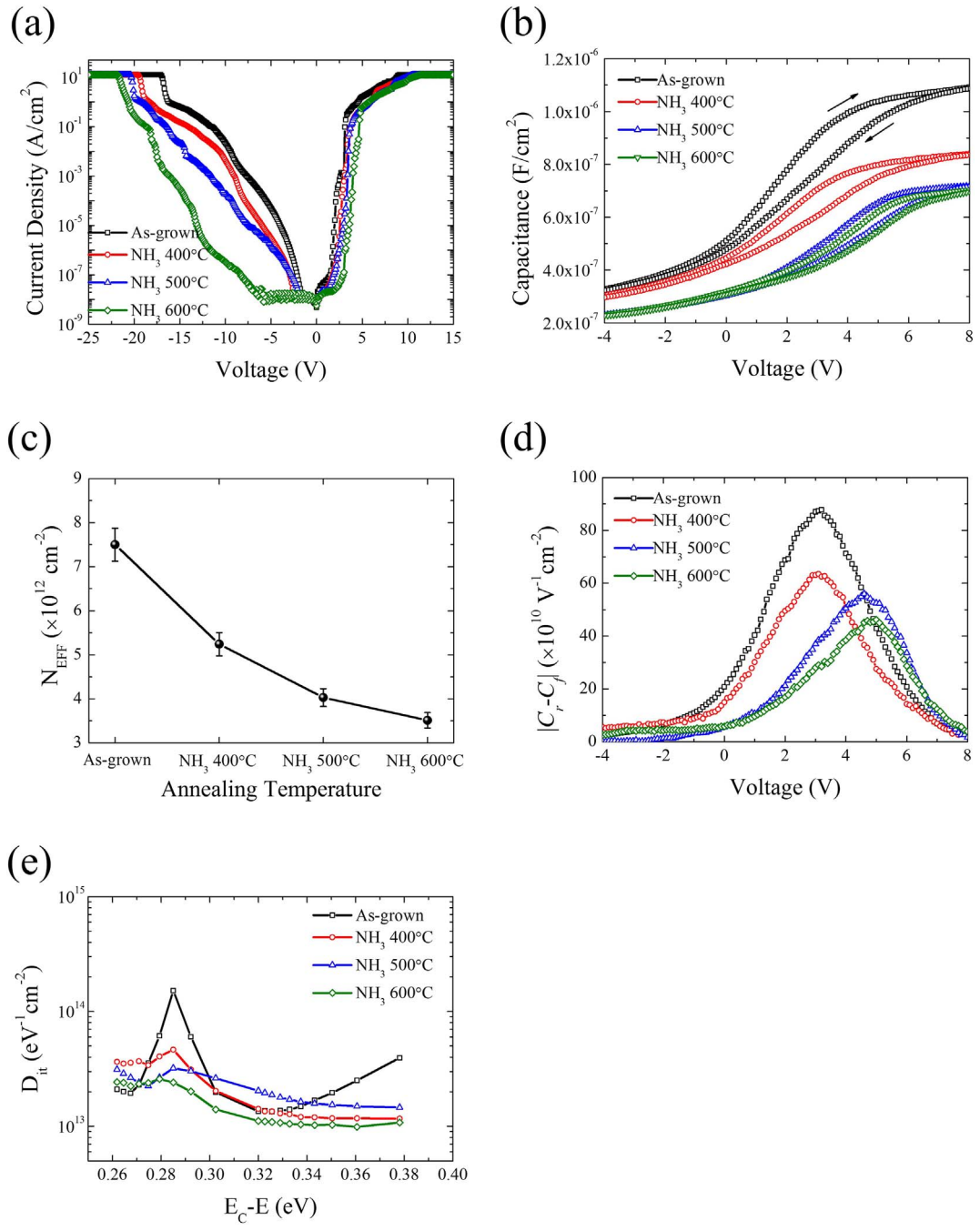

Fig. 4. (a) Leakage current density-voltage (J-V) characteristics, (b) capacitance-voltage (C-V) curves, (c) effective trap charge density (N_{EFF}), (d) effective border trap charge density, and (e) interface trap charge density (D_{it}) of the HfO_2/SiC as a function of the post-nitridation temperature.

conduction band and the band edge states was performed according to the normalization and Gaussian fits of the absorption spectra that were based on the second derivate analysis. Based on the local atomic bonding symmetry, the O *K*-edge absorption spectra of the HfO_2 directly reflect the molecular orbital hybridization between Hf with 5*d*, 6 *s*, and 6*p* and O with 2*p* [24]. The two distinct absorption peaks of the Hf 5*d* states are the e_g and t_{2g} states that are associated with the Hf 5*d* states. Beyond the Hf 5*d* states, the two broad peaks are denoted as a_{1g} and t_{1u} states that are associated with the Hf 6 *s* and 6*p* states, respectively [25]. The feature of the conduction band was maintained regardless of the nitridation temperature, which means that there were no changes of the micro-structure of the HfO_2 film. Fig. 3 (b) shows the defect states below the conduction band edge over a narrow energy region. The Gaussian fits identified two different types of defect states that are located at similar energies below the Hf 5*d* e_g conduction band edge. According to the equivalent d^4–d^{4*} transition state for the O divacancy, the origin of these peaks could be the defect states below the conduction band edge [24]. More specifically, the D1 state is caused by the Hf^{3+} states that are associated with an O divacancy by Hf_2O_3, while the D2 state is the result of an O divacancy in the HfO_2 film [26,27]. To exactly compare the quantitative magnitude of the two defect states, the relative defect absorption areas of the D1 and D2 are indicated in Fig. 3 (c). As the post-nitridation temperature was increased, the band edge states for the D1 and D2 decreased, and the minimum values of the intensities of two peaks occurred while the post-annealing temperature increased up to 600 °C. This decrease of the band edge states could induce a charge trapping reduction.

As previously stated, the electrical characteristics were examined

using the J-V and C-V. Fig. 4 (a) shows the J-V characteristics as a function of the post-nitridation temperature. The breakdown voltages of the as-grown HfO_2/SiC were − 17.1 V and 9.1 V under the negative and positive bias, respectively. With the post-nitridation temperature increased up to 600 °C, the breakdown voltages increased to − 21.8 V and 11.2 V, respectively. Even if the thickness of the interfacial layer was increased by the increasing of the post-nitridation temperature, the improvement of leakage current characteristics under the negative and positive biases could be associated with the decreasing of the defect states below the conduction band edge. In addition, the improvement of the leakage current density and the breakdown voltage was related to the decreasing of the carrier injection that is due to the higher ΔE_{VB} and ΔE_{CB} values at the post-nitridation temperature of 600 °C. Fig. 4 (b) shows the C-V hysteresis characteristics of the HfO_2/SiC that were measured at 1 MHz as a function of the post-nitridation temperature. The dielectric constant (k) calculated from the capacitance in the accumulation region for as-grown HfO_2/SiC is 12.3 and the value of k is 11.2, 11.6, and 11.6 with increasing the post-nitridation temperature of 400, 500, and 600 °C, respectively. The C-V hysteresis exhibited a clockwise hysteresis loop regardless of the post-annealing temperature, and that is related to the electron trapping in the oxide layer [26]. From the C-V hysteresis characteristics of the HfO_2/SiC, we calculated the effective trap charge density by using $N_{EFF} = \frac{C_{OX}\Delta V_{FB,hysteresis}}{qA}$, where C_{OX} is the capacitance of the oxide layer, $\Delta V_{FB,hysteresis}$ is the hysteresis in the flat band voltage, q is the electron charge, and A is the electrode area [28]. The calculated effective trap charge density is plotted in Fig. 4 (c), and the HfO_2/SiC with the post-nitridation temperature at 600 °C has minimum value ($3.51 \times 10^{12}\,cm^{-2}$). Also, we extracted the effective border trap density from the C-V hysteresis characteristics, as shown in Fig. 4 (d). The effective border trap density was calculated from the difference of the capacitance values between the forward and reverse voltage sweeps, $C_{rf}(V_g) = |C_r - C_f|$, where C_r and C_f are the capacitance during the reverse and forward sweeps, respectively. The shift of C-V curve indicates the electron trapping process occurred near the interface region in HfO_2/SiC. This result shows that the effective border trap of HfO_2/SiC ($4.61 \times 10^9\,V^{-1}\,cm^{-2}$) with post-nitridation temperature at 600 °C is smaller than that of the as-grown HfO_2/SiC ($8.77 \times 10^9\,V^{-1}\,cm^{-2}$). It could be related to the slow traps located at the interfacial region between oxide layer and the interfacial transition layer near the SiC substrate. Therefore, the high border trap density could be induced by formation of oxygen vacancies and interfacial layer at the interface region. These defects influence the charge trapping and detrapping process and result in large C-V hysteresis. In addition, the interface trap density (D_{it}) was compared as a function of the post-nitridation temperature and the results were plotted in Fig. 4 (e). To determine the D_{it} in the HfO_2/SiC, the capacitance (C_m) and the conductance (G_m) were measured at different frequencies (f) in a parallel mode. The D_{it} and the trap level energy position were calculated from the parallel conductance $(G_p/\omega)_{max}$ by using a combination of the forward bias capacitance-frequency (*C-f*) and conductance-frequency (*G-f*) [29]. The G_p/ω value was calculated by the equation below

$$\frac{G_p}{\omega} = \frac{\omega G_m C_{ox}^2}{G_m^2 + \omega^2 (C_{ox} - C_m)^2}$$

where ω is $2\pi f$ (f is the measurement frequency from 10 kHz to 1 MHz), C_{ox} is the accumulation capacitance value, and G_m and C_m are the measured conductance and capacitance, respectively. The D_{it} in the depletion region is proportional to the value of $(G_p/\omega)_{max}$ and the equation of D_{it} can be estimated by the following equation

$$D_{it} \approx 2.5 \frac{(G_p/\omega)_{max}}{Aq}$$

where A is the area of the electrode and q is the elemental charge. HfO_2/SiC with the post-nitridation temperature at 600 °C showed a lower D_{it} value ($\sim 2.6 \times 10^{-13}\,eV^{-1}\,cm^{-2}$), compared to the other sample. These D_{it} distribution results are closely related to the interfacial trap states near the SiC substrate. The decrease of D_{it} is caused by the reduction of interfacial states via incorporation of nitrogen at the interface of HfO_2/SiC, as shown in the previous results for the increase of band offset and the decrease of band edge states.

4. Conclusions

In summary, the evolution of the defect states below the conduction band of the HfO_2/SiC has been reported according to the effect of nitrogen incorporation into HfO_2 films and as a function of the post-annealing temperature in the NH_3 ambient. The band offsets of the conduction band and the valence band between the HfO_2 and SiC were slightly increased, and the band edge states below the conduction band were dramatically decreased with the increase of the post-nitridation temperature. The leakage characteristics were improved, and the trap density at the films and the interface were reduced with the increase of post-nitridation temperature. Therefore, the insulating properties of HfO_2 on SiC substrate could be improved by the reduction of defect states using a post-nitridation treatment in the NH_3 ambient.

Acknowledgement

This work was supported by National Research Foundation Grant (NRF-2014M2B2A4030839) from the Ministry of Science, ICT and Future Planning (MSIP) of the Republic of Korea.

References

[1] T. Kimoto, Material science and device physics in SiC technology for high-voltage power devices, Jpn. J. Appl. Phys. 54 (2015) 040103.
[2] J. Spizt, M.R. Melloch, J.A. Cooper, M.A. Capano, 2.6 kV 4H-SiC lateral DMOSFET's, IEEE Electron Device Lett. 19 (1998) 100–102.
[3] Philip G. Neudeck, Progress in silicon carbide semiconductor electronics technology, J. Electron. Mater. 24 (1995) 283–288.
[4] G. Gudjónsson, H.Ö. Ólafsson, F. Allerstam, P.-Å. Nilsson, E.Ö. Sveinbjörnsson, H. Zirath, T. Rödle, R. Jos, High field-effect mobility in n-channel Si face 4H-SiC MOSFETs with gate oxide grown on aluminum ion-implanted material, IEEE Electron Device Lett. 26 (2005) 96–98.
[5] P. Jamet, S. Dimitrijev, P. Tanner, Effects of nitridation in gate oxides grown on 4H-SiC, J. Appl. Phys. 90 (2001) 5058–5063.
[6] Lori A. Lipkin, John W. Palmour, Insulator investigation on SiC for improved reliability, IEEE Trans. Electron Devices 46 (1999) 525–532.
[7] L.M. Lin, P.T. Lai, Improved high-field reliability for a SiC metal-oxide-semiconductor device by the incorporation of nitrogen into its HfTiO gate dielectric, J. Appl. Phys. 102 (2007) 054515.
[8] S.S. Hullavarad, D.E. Pugel, E.B. Jones, R.D. Vispute, T. Venkatesan, Low leakage current transport and high breakdown strength of pulsed laser deposited HfO_2/SiC metal-insulator-semiconductor device structures, J. Electron. Mater. 36 (2007) 648–653.
[9] V.V. Afanas'ev, A. Stesmans, F. Chen, S.A. Campbell, R. Smith, HfO_2-based insulating stacks on 4H-SiC (0001), Appl. Phys. Lett. 82 (2003) 922–924.
[10] V.V. Afanas'ev, F. Ciobanu, S. Dimitrijev, G. Pensl, A. Stesmans, Band alignment and defect states at SiC/oxide interfaces, J. Phys. Condens. Matter 16 (2004) S1839–S1856.
[11] G. Chung, C.C. Tin, J.R. Williams, K. McDonald, M. Di Ventra, R.K. Chanana, S.T. Pantelides, L.C. Feldman, R.A. Weller, Effects of anneals in ammonia on the interface trap density near the band edges in 4H-silicon carbide metal-oxide-semiconductor capacitors, Appl. Phys. Lett. 77 (2000) 3601–3603.
[12] X. Zhu, A.C. Ahyi, M. Li, Z. Chen, J. Rozen, L.C. Feldman, J.R. Wiliams, The effect of nitrogen plasma anneals on interface trap density and channel mobility for 4H-SiC MOS devices, Solid State Electron. 57 (2011) 76–79.
[13] H. Li, S. Dimitrijev, H.B. Harrison, D. Sweatman, Interfacial characteristics of N_2O and NO nitride SiO_2 grown on SiC by rapid thermal processing, Appl. Phys. Lett. 70 (15) (1997) 2028–2030.
[14] A. Poggi, F. Moscatelli, S. Solmi, R. Nipoti, Investigation on the use of nitrogen implantation to improve the performance of n-channel enhancement 4H-SiC MOSFETs, IEEE Trans. Electron Devices 55 (2008) 2021–2028.
[15] G. Pensl, S. Beljakowa, T. Frank, K. Gao, F. Speck, T. Seyller, L. Ley, F. Ciobanu, V. Afanas'ev, A. Stesmans, T. Kimoto, A. Schoner, Alternative techniques to reduce interface traps in n-type 4H-SiC MOS capacitors, Phys. Status Solidi B 245 (2008) 1378–1389.
[16] K. McDonald, R.A. Weller, L.C. Feldman, J.R. Williams, F.C. Stedile, I.J.R. Baumvol, C. Radtke, Comparison of nitrogen incorporation in SiO_2/SiC and SiO_2/Si structures, Appl. Phys. Lett. 76 (5) (2000) 568–570.
[17] J. Rozen, S. Dhar, M.E. Zvanut, J.R. Williams, L.C. Feldman, Density of interface states, electron traps, and hole traps as a function of the nitrogen density in SiO_2 on

SiC, J. Appl. Phys. 105 (2009) 124506.
[18] S. Dhar Sanwu Wang, Shu-rui Wang, A.C. Ahyi, A. Franceschetti, J.R. Williams, L.C. Feldman, Sokrates T. Pantelides, Bonding at the SiC-SiO_2 interface and the effects of nitrogen and hydrogen, Phys. Rev. Lett. 98 (2007) 026101.
[19] J. Rozen, M. Nagano, H. Tsuchida, Enhancing interface quality by gate dielectric deposition on a nitrogen-conditioned 4H-SiC surface, J. Mater. Res. 28 (2013) 28–32.
[20] M. Dai, Y. Wang, J. Shepard, J. Liu, M. Brodsky, S. Siddiqui, P. Ronsheim, D.P. Ioannou, C. Reddy, W. Henson, S. Krishnan, V. Narayanan, M.P. Chudzik, Effect of plasma N_2 and thermal NH_3 nitridation in HfO_2 for ultrathin equivalent oxide thickness, J. Appl. Phys. 113 (2013) 044103.
[21] M.-H. Cho, K.B. Chung, C.N. Whang, D.-H. Ko, J.H. Lee, N.I. Lee, Nitridation for HfO_2 high-k films on Si by an NH_3 annealing treatment, Appl. Phys. Lett. 88 (2006) 202902.
[22] J.G. Chen, NEXAFS investigations of transition metal oxides, nitrides, carbides, sulfides and other interstitial compounds, Surf. Sci. Rep. 30 (1997) 1–152.
[23] C.J. Yim, D.–.H. Ko, S.H. Park, W.J. Lee, M.–.H. Cho, Effect of incorporated nitrogen on the band alignment of ultrathin silicon-oxynitride films as a function of the plasma nitridation conditions, J. Korean Phys. Soc. 58 (5) (2011) 1169–1173.
[24] C.Y. Kim, K.S. Jeong, Y.S. Kang, S.W. Cho, M.-H. Cho, K.B. Chung, D.-H. Ko, Y. Yi, H. Kim, Defect states in epitaxial HfO_2 films induced by atomic transport from n-GaAs (100) substrate, J. Appl. Phys. 109 (2011) 114112.
[25] H. Jin, S.K. Oh, H.J. Kang, S.W. Lee, Y.S. Lee, M.H. Cho, Temperature dependence of band alignment in ultra-thin HfO_2/Si interface, J. Surf. Analysis 12 (2005) 254–257.
[26] K.B. Chung, J.P. Long, H. Seo, G. Lucovsky, D. Nordlund, Thermal evolution and electrical correlation of defect states in Hf-based high-k dielectrics on n-type Ge (100): Local atomic bonding symmetry, J. Appl. Phys. 106 (2009) (074102).
[27] K.-H. Xue, P. Blaise, L.R.C. Fonseca, G. Molas, E. Vianello, B. Traore, B. De Salvo, G. Ghibaudo, Y. Nishi, Grain boundary composition and conduction in HfO_2:An ab initio study, Appl. Phys. Lett. 102 (2013) 201908.
[28] P.–.C. Jiang, J.S. Chen, Effects of post-metal annealing on electrical characteristics and thermal stability of W_2N/Ta_2O_5/Si MOS capacitors, J. Electrochem. Soc. 151 (11) (2004) G751–G755.
[29] R.E. Herbert, Y. Hwang, S. Stemmer, Comparison of methods to quantify interface trap densities at dielectric/III-V semiconductor interfaces, J. Appl. Phys. 108 (2010) 124101.